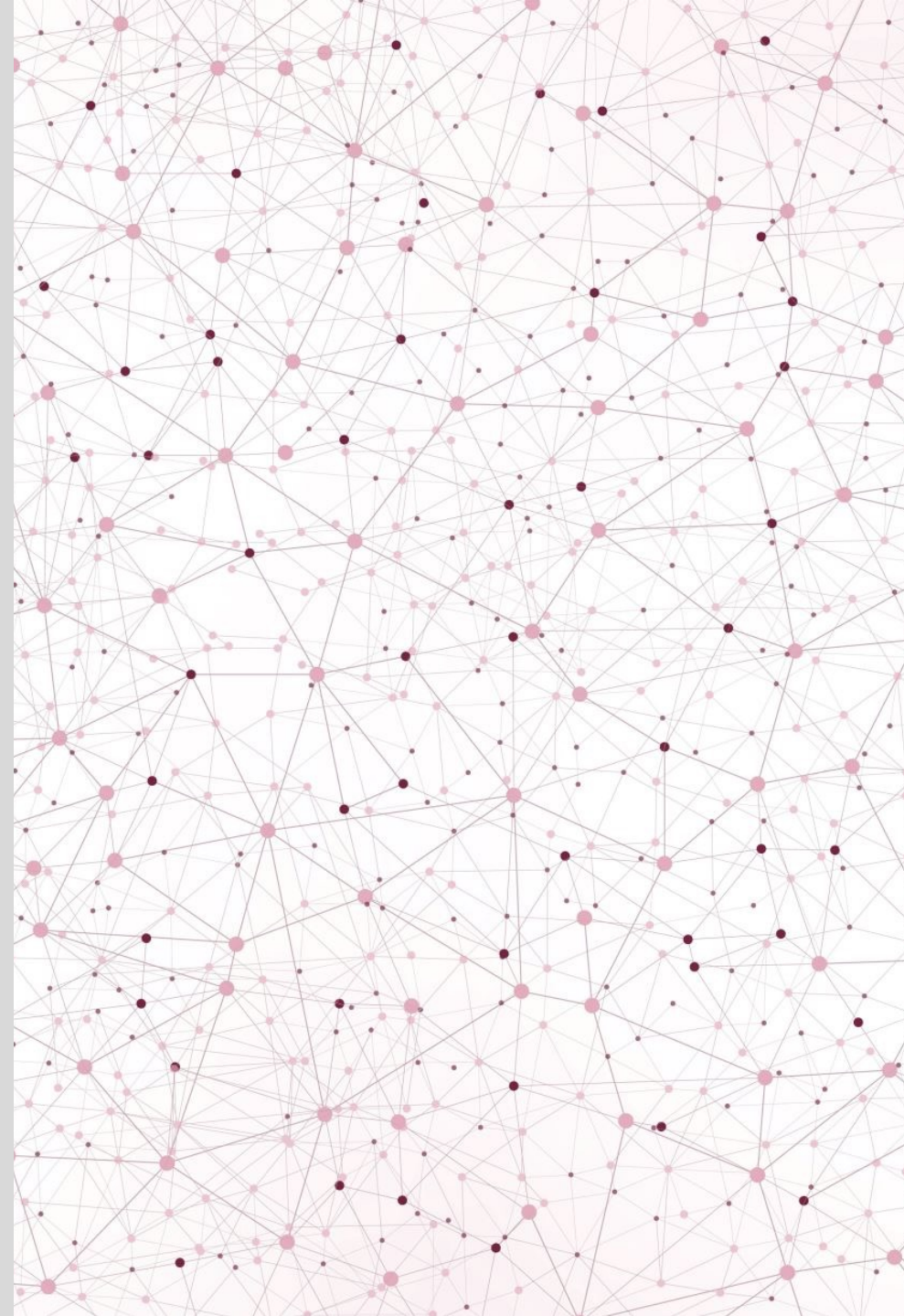




# CE $\nu$ NS BOUNDS ON NEUTRINO ELECTROMAGNETIC PROPERTIES

Francesca Dordei,  
[francesca.dordei@cern.ch](mailto:francesca.dordei@cern.ch)  
INFN Cagliari

Magnificent CE $\nu$ NS 2023, 22-24 of March, Munich



## Impact of the Dresden-II and COHERENT neutrino scattering data on neutrino electromagnetic properties and electroweak physics

M. Atzori Corona,<sup>a,b</sup> M. Cadeddu,<sup>b</sup> N. Cargioli,<sup>a,b</sup> F. Dordei,<sup>b</sup> C. Giunti,<sup>c</sup> Y.F. Li,<sup>d,e</sup> C.A. Ternes,<sup>c</sup> and Y.Y. Zhang<sup>d,e</sup>

<sup>a</sup>*Dipartimento di Fisica, Università degli Studi di Cagliari, Complesso Universitario di Monserrato, S.P. per Sestu Km 0.700, 09042 Monserrato (CA), Italy*

<sup>b</sup>*Istituto Nazionale di Fisica Nucleare (INFN), Sezione di Cagliari, Complesso Universitario di Monserrato, S.P. per Sestu Km 0.700, 09042 Monserrato (CA), Italy*

<sup>c</sup>*Istituto Nazionale di Fisica Nucleare (INFN), Sezione di Torino, Via P. Giuria 1, I-10125 Torino, Italy*

<sup>d</sup>*Institute of High Energy Physics, Chinese Academy of Sciences, Beijing 100049, China*

<sup>e</sup>*School of Physical Sciences, University of Chinese Academy of Sciences, Beijing 100049, China*

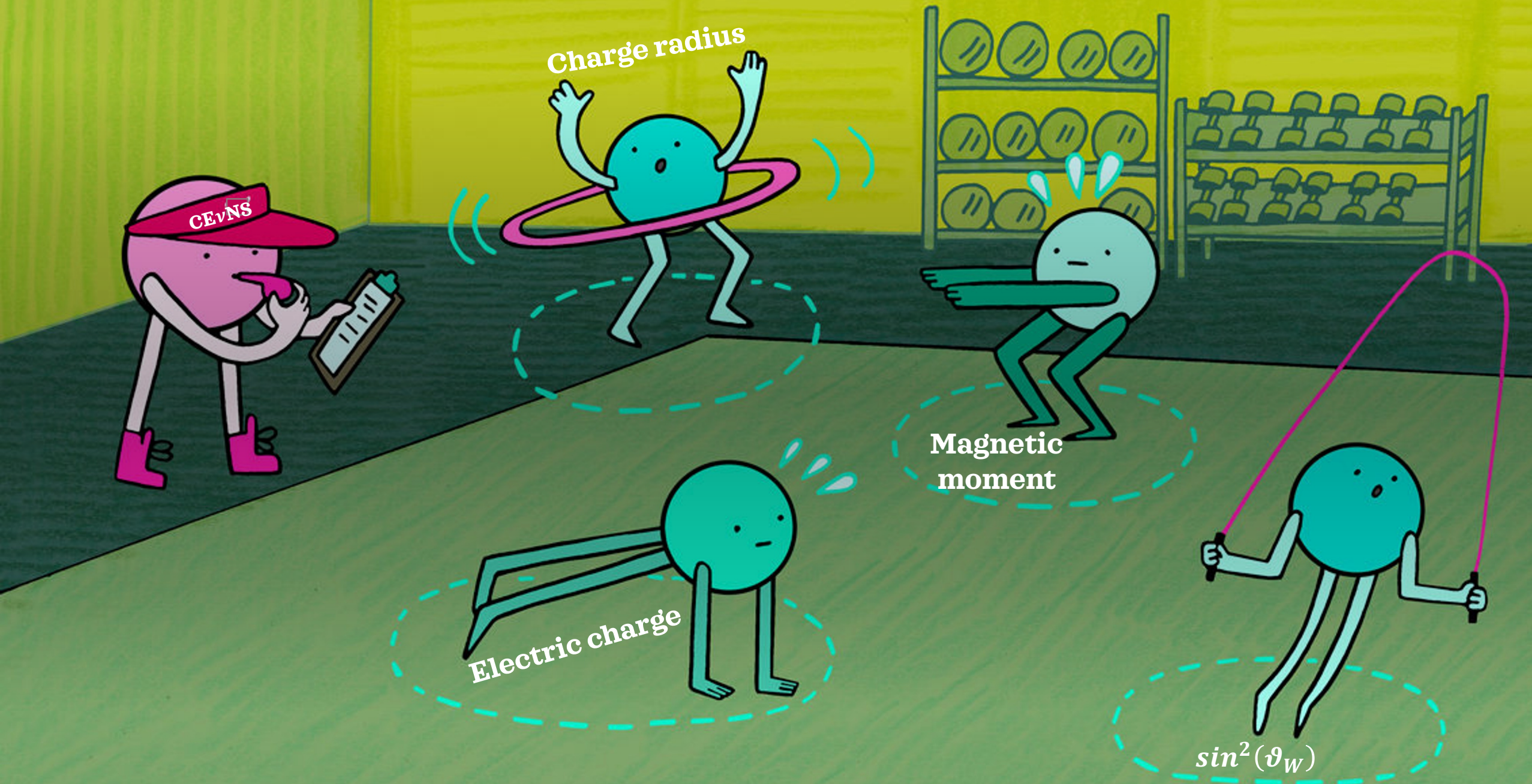
E-mail: [mattia.atzori.corona@ca.infn.it](mailto:mattia.atzori.corona@ca.infn.it), [matteo.cadeddu@ca.infn.it](mailto:matteo.cadeddu@ca.infn.it), [nicola.cargioli@ca.infn.it](mailto:nicola.cargioli@ca.infn.it), [francesca.dordei@cern.ch](mailto:francesca.dordei@cern.ch), [carlo.giunti@to.infn.it](mailto:carlo.giunti@to.infn.it), [liyufeng@ihep.ac.cn](mailto:liyufeng@ihep.ac.cn), [ternes@to.infn.it](mailto:ternes@to.infn.it), [zhangyiyu@ihep.ac.cn](mailto:zhangyiyu@ihep.ac.cn)

**ABSTRACT:** Coherent elastic neutrino-nucleus scattering (CE $\nu$ NS) represents a powerful tool to investigate key electroweak physics parameters and neutrino properties since its first observation in 2017 by the COHERENT experiment exploiting the spallation neutron source at Oak Ridge National Laboratory. In light of the recent detection of such a process with antineutrinos produced by the Dresden-II reactor scattering off a germanium detector, we revisit the limits so far set on the neutrino magnetic moments, charge radii and millicharges as well as on the weak mixing angle. In order to do so, we also include the contribution of elastic neutrino-electron scattering, whose effect becomes non negligible in some beyond the Standard Model theories. By using different hypotheses for the germanium quenching factor and the reactor antineutrino flux, we provide a measurement of the weak mixing angle at the low-energy scale of the Dresden-II reactor experiment and, thanks to a combined analysis with the latest cesium iodide and argon data set released by the COHERENT Collaboration, we deliver updated limits for the neutrino electromagnetic

BASED ON  
JHEP09(2022)164

[https://doi.org/10.1007/JHEP09\(2022\)164](https://doi.org/10.1007/JHEP09(2022)164)

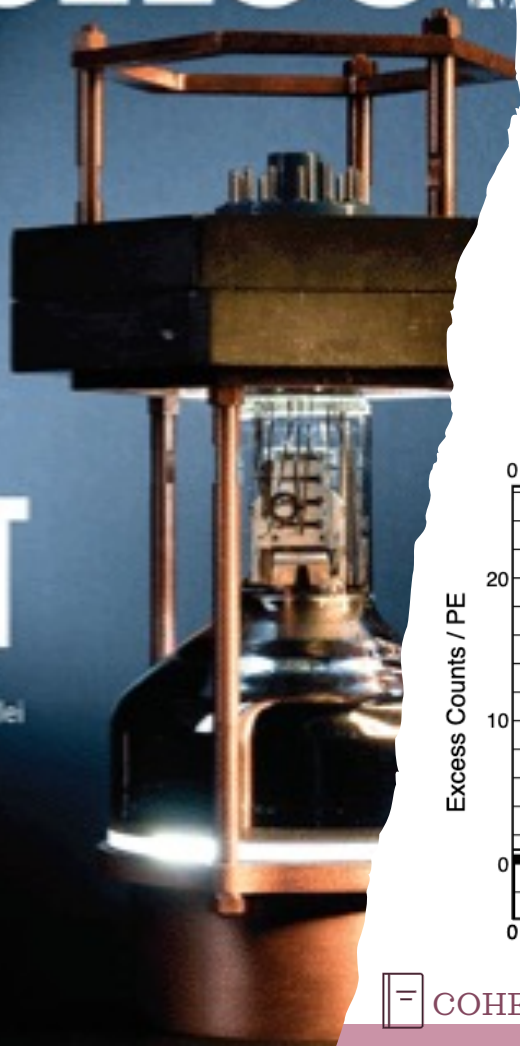
Done in collaboration with: **M. Atzori Corona, M. Cadeddu, N. Cargioli**, C. Giunti, Y.F. Li, C.A. Ternes and Y.Y. Zhang



# Science

## SPOTTING A GHOST

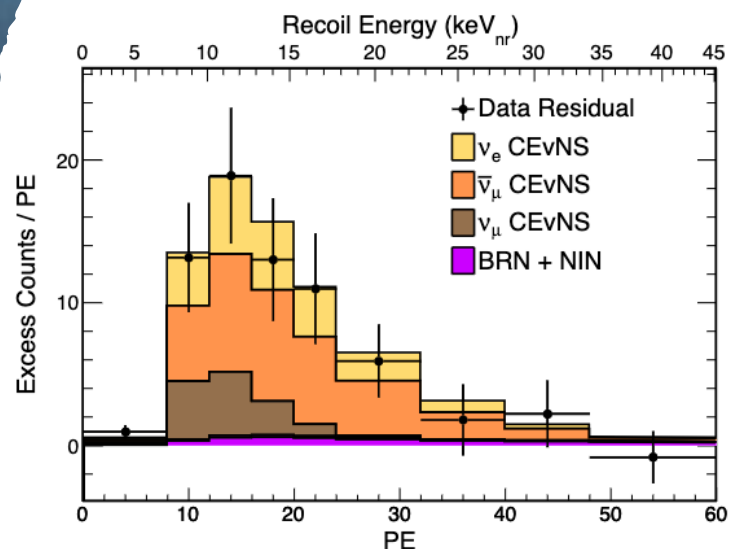
A compact detector spies  
neutrinos scattering from nuclei  
pp. 1098 & 1123



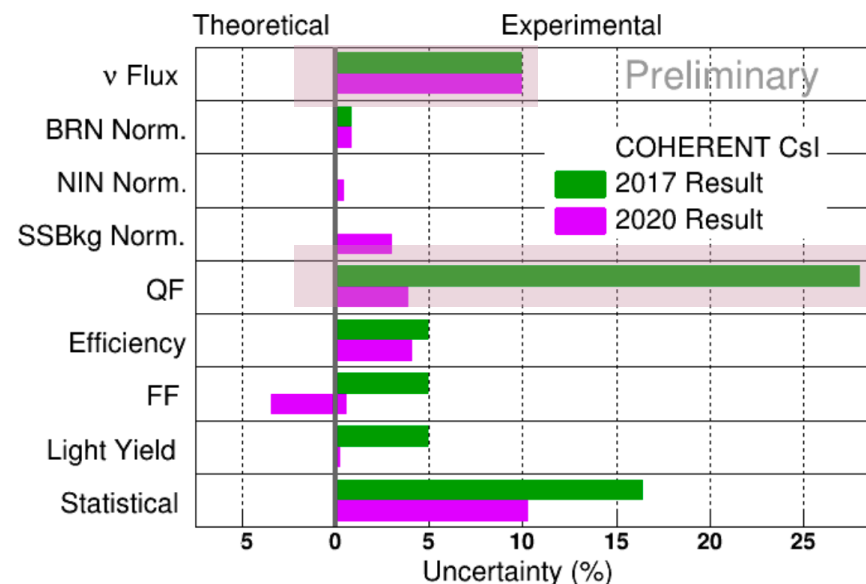
## Leading actor I



- Full CEvNS dataset with 14.6 kg CsI scintillating crystal and neutrinos from  $\pi$ DAR
- **$306 \pm 20$  CEvNS** events:  $11.6\sigma$  significance
- To be compared with prediction:  **$333 \pm 11$ (th)  $\pm 42$ (ex)** events
- ✓ Result is consistent with SM prediction at  $1\sigma$
- ✓ Double exposure wrt 2017 and updated quenching factor model
- ✓ Flux uncertainty now dominates the systematic uncertainty.
- ✓ Overall systematic uncertainty reduced: 28%  $\rightarrow$  13%



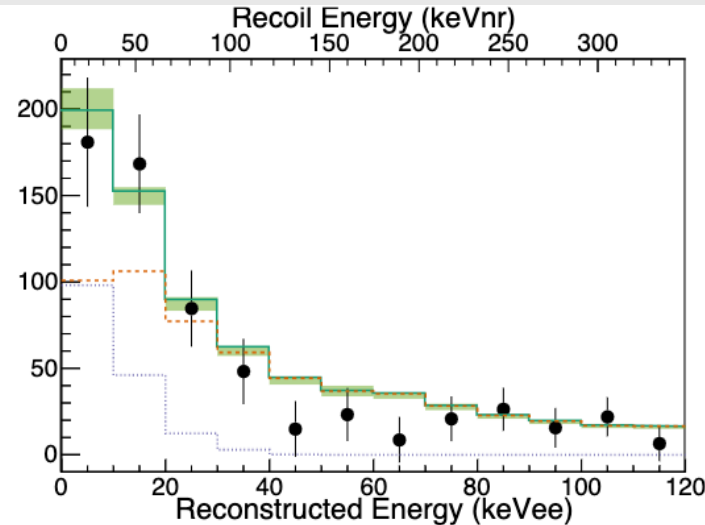
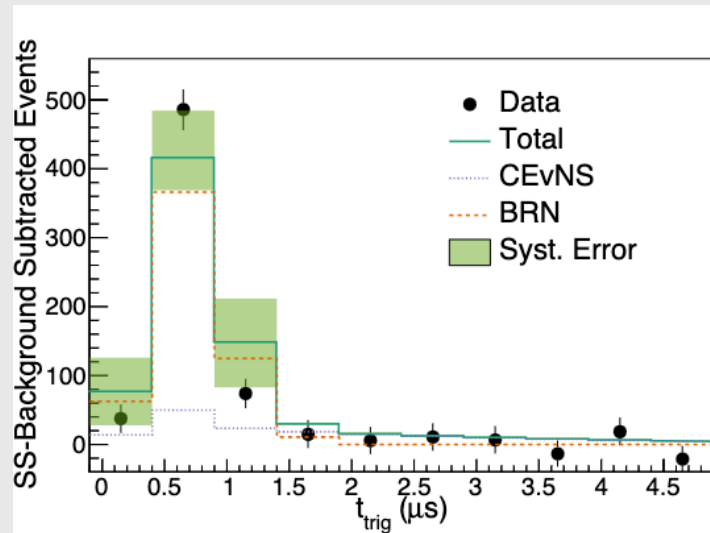
COHERENT, PRL 129, 081801 (2022)



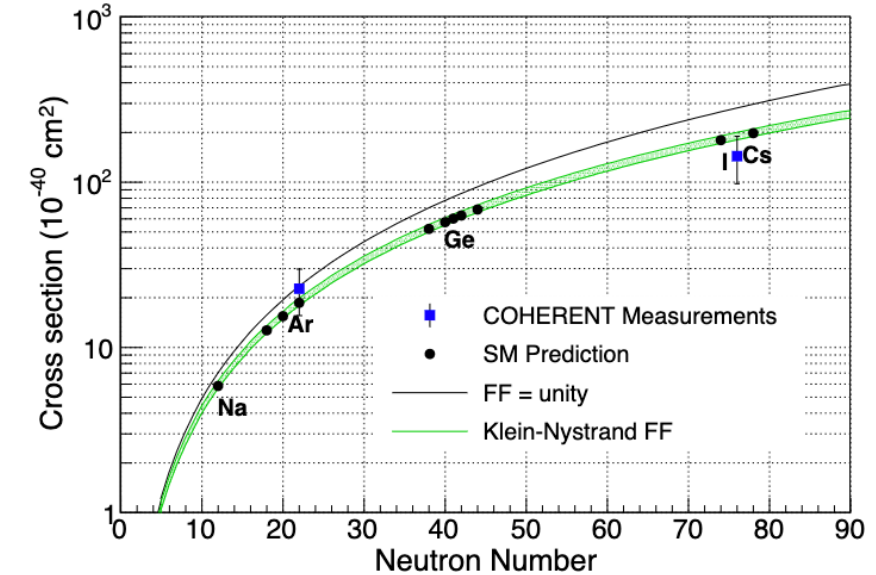
# Leading actor II



- 2020 first results using Ar, aka CENNS-10.
- Active mass of 24 kg of atmospheric argon
- Single phase only (scintillation), thr.  $\sim 20 \text{ keV}_{\text{nr}}$
- ✓ Two independent analyses observed a more than  $3\sigma$  excess over background
- ✓ Still collecting data, more precise results expected soon.



Verify the **expected neutron-number dependence** of cross-section



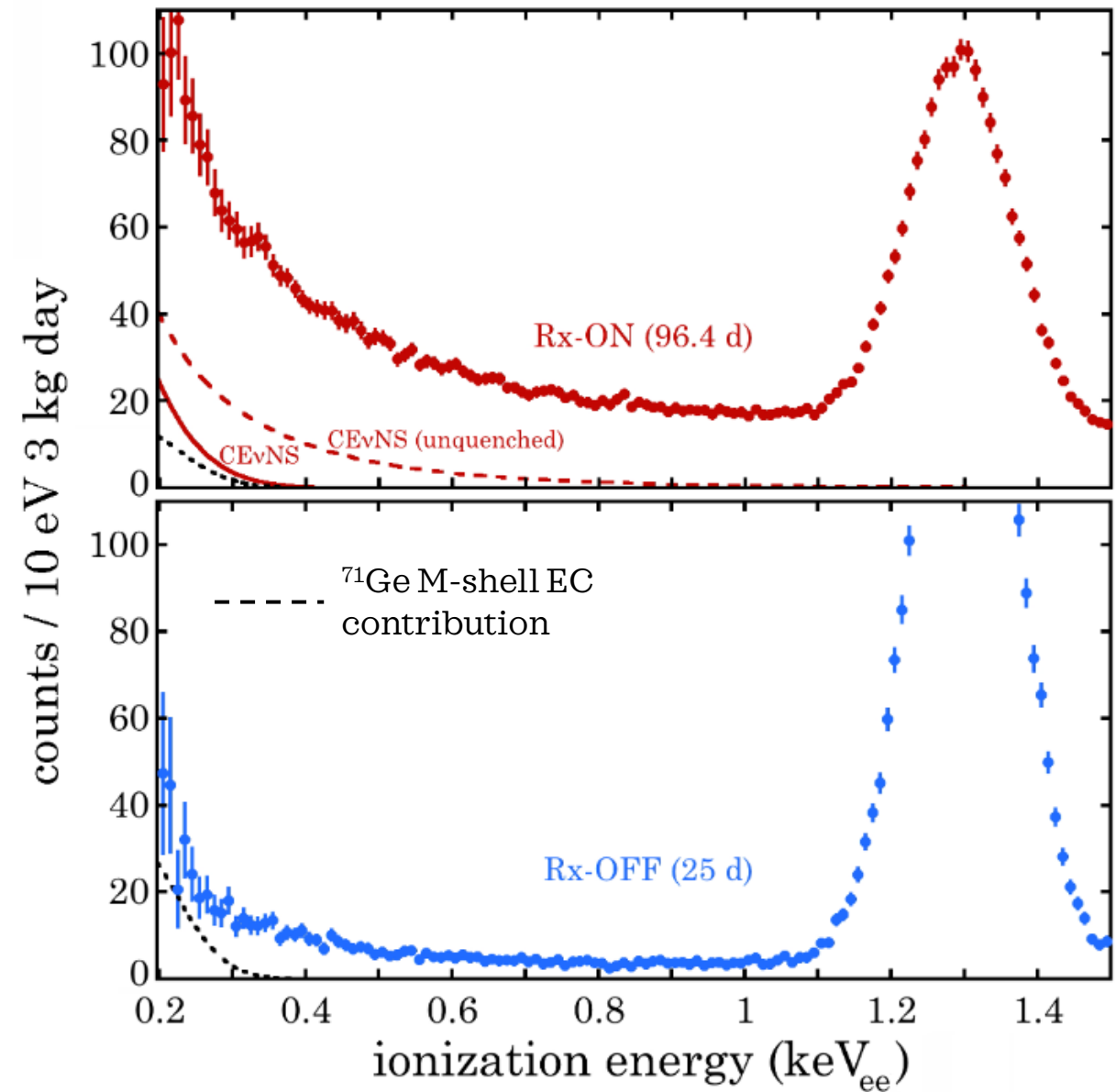
The form factor unity assumption is compared to the Klein-Nystrand value that is used for this analysis with the green band representing a  $\pm 3\%$  variation on the neutron radius.

COHERENT, PRL 126, 012002 (2021)

# Leading actor III



- 96.4 day (**Rx-ON**) exposure of a 3 kg ultra-low noise germanium detector (NCC-1701)
  - 10.39 m away from the Dresden-II boiling water reactor (P=2.96Gw<sub>th</sub>)
  - **Low energy threshold:** 0.2 keV<sub>ee</sub>
  - 25 days of reactor off (**Rx-OFF**)
  - The background comes from the elastic scattering of **epithermal neutrons** and the **electron capture in <sup>71</sup>Ge**
- $$\frac{dN^{\text{bkg}}}{dT_e} = \overbrace{N_{\text{epith}} + A_{\text{epith}} e^{-T_e/T_{\text{epith}}}} + \overbrace{\sum_{i=L1,L2,M} \frac{A_i}{\sqrt{2\pi}\sigma_i} e^{-\frac{(T_e-T_i)^2}{2\sigma_i^2}}}$$
- **Strong preference** (p<1.2x10<sup>-3</sup>) for the presence of CEνNS is found, when compared to a background-only model.



# Germanium quenching factor

The electron-equivalent recoil energy  $T_e$ , observed in the detector, is transformed into the nuclear recoil energy  $T_{nr}$  in the CEvNS rate by inverting the relation

$$T_e = f_Q(T_{nr}) T_{nr} \quad \text{Quenching factor}$$

For germanium, for consistency with the Dresden-data we consider two models based on experimental measurements taken from [PRL 129, 211802 \(2022\)](#)

- from **photo-neutron source measurements** (YBe)
- from **iron-filtered monochromatic neutrons**, (Fef), that consists in a simple linear fit of the four data points for  $T_{nr} \leq 1.35$  keV and is extended above this range with the standard Lindhard model with  $k = 0.157$ .

 [Collar et al, PRD 103, 122003 \(2021\)](#)

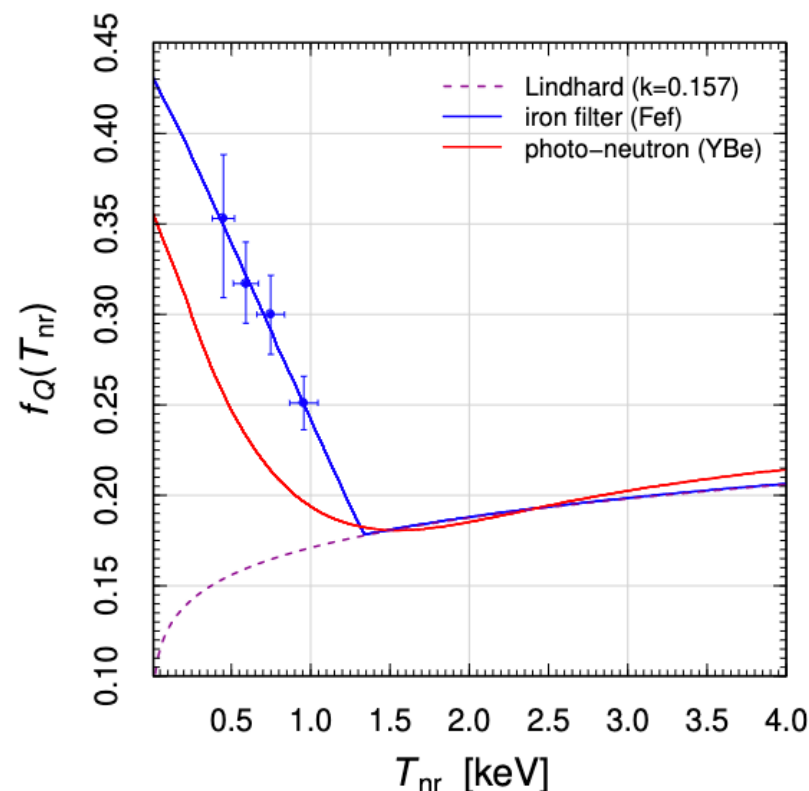


Very **debated within the community**: see W. Maneshg talk on “*Recent results from the CONUS experiment*”. CONUS data are compatible with the Lindhard theory with a parameter  $k$  of  $0.162 \pm 0.004$  (stat+sys).

**Tension with Dresden-II results.**

 [CONUS Coll., Eur. Phys. J. C 82, 815 \(2022\)](#)

 [Lindhard et al, Notes on atomic collisions \(1963\)](#)



# CONS

- **Antineutrinos @nuclear power reactors:** larger background without pulsed source, less significant CEvNS signal.
- **Lower neutrino energy in combination with low en. thresholds:** no information available on  $R_n$ .
- Results very sensitive to the **Germanium quenching factor parametrization** used.
  - ➔ Needs to clarify measurements at low energies.
- Absence of muon neutrinos: **some BSM theories/parameters can not be studied.**

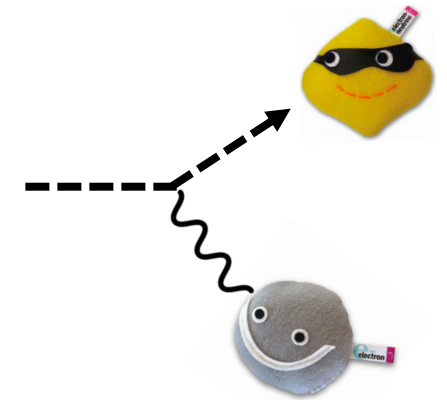
## Why including Dresden-II (reactor) data?



# PROS

- **Antineutrinos @nuclear power reactors:** continuous and well-localized source, intense fluxes, low energy.
- **Lower neutrino energy in combination with low en. thresholds:** negligible dependence on  $R_n$  (robust limits)
- Provide a **weak mixing angle** measurement at lower energies independent from  $R_n$ .
- Dependence on  $1/T_e$  of some new physics scenarios allows us to put **more stringent limits** (e.g. neutrino magnetic moment)

# ELASTIC $\nu$ –ELECTRON SCATTERING



- $\nu$ -electron elastic scattering (ES) is a **concurrent process to CEvNS**
- In the SM, its contribution to the total event rate is small and can be neglected
- **In certain BSM scenarios the ES contribution increases significantly** ➡ Allows us to achieve stronger constraints !

$$\frac{d\sigma^{ES}(E_\nu, T_e)}{dT_e} = Z_{eff}^A(T_e) \frac{G_F^2 m_e}{2\pi} \left[ (g_V^{\nu_l} + g_A^{\nu_l})^2 + (g_V^{\nu_l} - g_A^{\nu_l})^2 \left(1 - \frac{T_e}{E_\nu}\right)^2 - ((g_V^{\nu_l})^2 - (g_A^{\nu_l})^2) \frac{m_e T_e}{E_\nu^2} \right]$$

Neutrino energy  $\rightarrow$   $E_\nu$

Mass of the electron  $\rightarrow$   $m_e$

SM neutrino electron coupling  $\rightarrow$   $g_V^{\nu_l}, g_A^{\nu_l}$

Electron recoil energy  $\rightarrow$   $T_e$

$Z_{eff}^A(T_e)$  The interaction is not with free electrons but atomic electrons! Quantifies the **number of electrons that can be ionized by a certain energy deposit  $T_e$** .

$g_V^{\nu_e} = 2 \sin^2 \theta_W + 1/2, \quad g_A^{\nu_e} = 1/2,$   
 $g_V^{\nu_{\mu,\tau}} = 2 \sin^2 \theta_W - 1/2, \quad g_A^{\nu_{\mu,\tau}} = -1/2$  + radiative corrections

- The  $Z_{eff}^A(T_e)$  term is needed to correct the cross section derived under the Free Electron Approximation (FEA) hypothesis, where electrons are considered to be free and at rest (would just scale as Z).
- Alternative ab-initio approach: **multi-configuration relativistic random phase approximation** (MCRRPA) able to improve the description of the atomic many-body effects
- We do not include such contribution for Ar, where the  $f_{90}$  parameter removes electron recoils due to ES

☐ PRA 25 (1982) 634

The background of the slide is a blurred bokeh of colorful city lights in shades of yellow, orange, blue, and pink. In the center, a hand is holding a magnifying glass, which focuses on a clear image of a busy city street at night, likely Tokyo, showing tall buildings and numerous illuminated signs. The text 'NEUTRINO CHARGE RADII' is written in a white, serif font, centered over the magnifying glass and the city scene.

# NEUTRINO CHARGE RADII

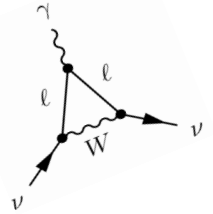
# Neutrino charge radius - theory

- In the SM, the neutrino charge radii (CR) are the **only electromagnetic properties of neutrinos that are different from zero**.
- The contribution of the SM neutrino CR is taken into account as one of the radiative corrections to  $g_V^p(\nu_\ell)$

$$\langle r_{\nu_\ell}^2 \rangle_{\text{SM}} = -\frac{G_F}{2\sqrt{2}\pi^2} \left[ 3 - 2 \ln \left( \frac{m_\ell^2}{m_W^2} \right) \right]$$

$$\langle r_{\nu_e}^2 \rangle_{\text{SM}} = -0.83 \times 10^{-32} \text{ cm}^2$$

$$\langle r_{\nu_\mu}^2 \rangle_{\text{SM}} = -0.48 \times 10^{-32} \text{ cm}^2$$



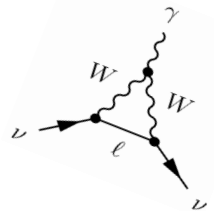
- In the SM CR are diagonal in the flavour basis, but in BSM also off-diagonal (transition) CR can be generated.

**CEvNS:**  $\frac{d\sigma_{\nu_\ell-\mathcal{N}}^{\text{CR}}}{dT_{\text{nr}}}(E, T_{\text{nr}}) = \frac{G_F^2 M}{\pi} \left( 1 - \frac{MT_{\text{nr}}}{2E^2} \right) \left\{ \left[ \left( \tilde{g}_V^p - \tilde{Q}_{\ell\ell} \right) ZF_Z(|\vec{q}|^2) + g_V^n NF_N(|\vec{q}|^2) \right]^2 + Z^2 F_Z^2(|\vec{q}|^2) \sum_{\ell' \neq \ell} |\tilde{Q}_{\ell\ell'}|^2 \right\}$

$\nu$ -proton coupling without the contribution of the SM CR

with  $\tilde{Q}_{\ell\ell'} = \frac{\sqrt{2}\pi\alpha}{3G_F} \langle r_{\nu_{\ell\ell'}}^2 \rangle$  Effective shift of the weak mixing angle

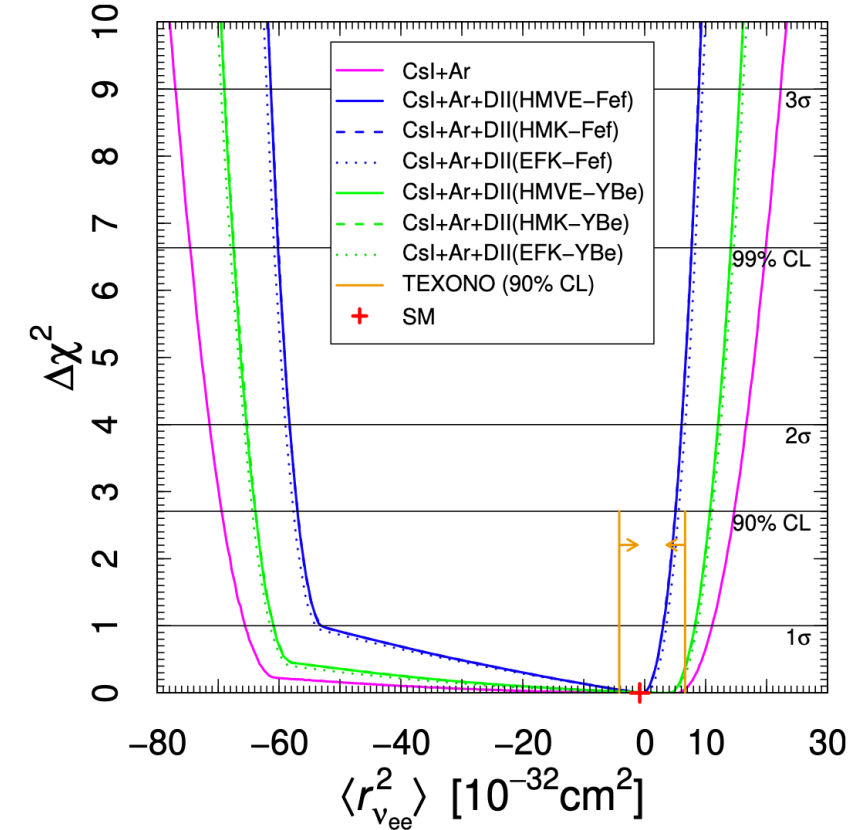
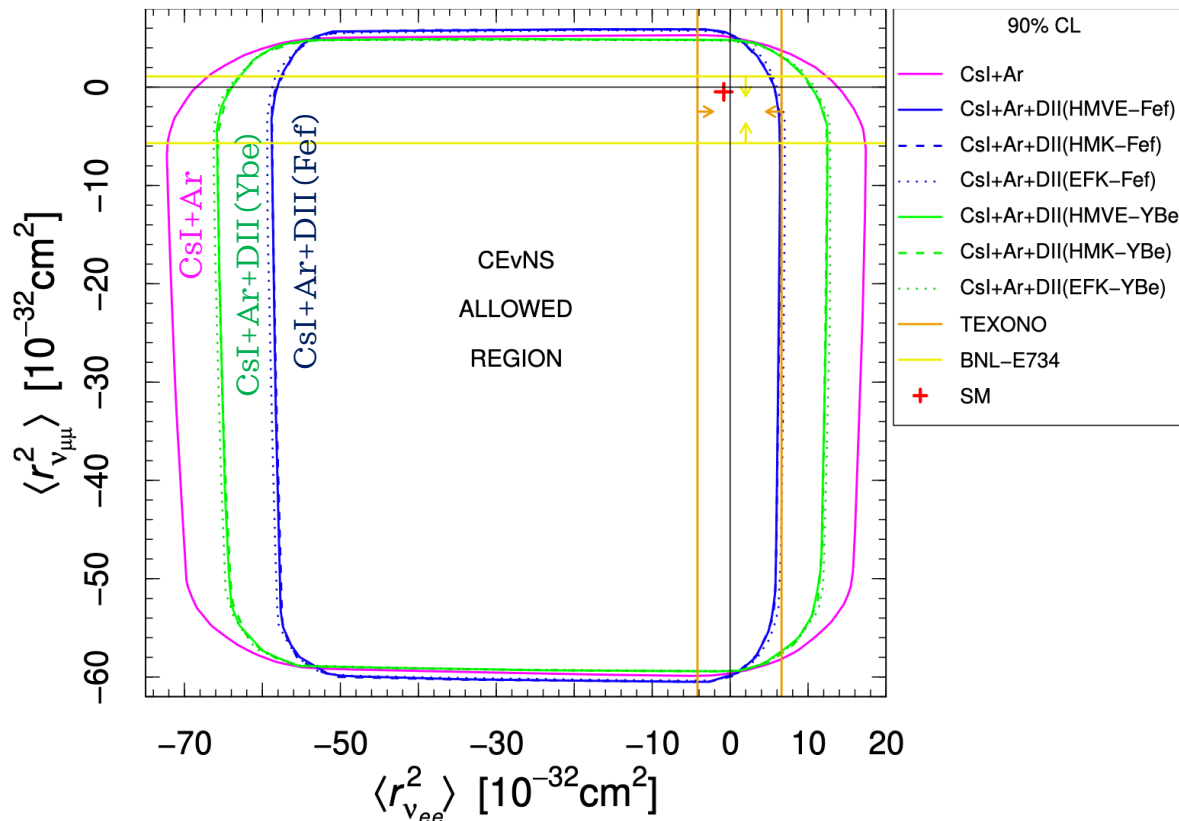
**ES:**  $\left( \frac{d\sigma_{\nu_\ell-\mathcal{A}}^{\text{ES,CR}}}{dT_e} \right)_{\text{SM}+\tilde{Q}} = \left( \frac{d\sigma_{\nu_\ell-\mathcal{A}}^{\text{ES,CR}}}{dT_e} \right)_{\text{SM}+\tilde{Q}_{\ell\ell}} + \sum_{\ell' \neq \ell} Z_{\text{eff}}^{\mathcal{A}}(T_e) \frac{\pi\alpha^2 m_e}{9} \left[ 1 + \left( 1 - \frac{T_e}{E} \right)^2 - \frac{m_e T_e}{E^2} \right] |\langle r_{\nu_{\ell\ell'}}^2 \rangle|^2$



**Current best limits:** accelerator  $\nu_{e/\mu} - e$  scattering. **TEXONO**  $-4.2 < \langle r_{\nu_e}^2 \rangle < 6.6 [10^{-32} \text{ cm}^2]$ , **BNL-E734**  $-5.7 < \langle r_{\nu_\mu}^2 \rangle < 1.1 [10^{-32} \text{ cm}^2]$  @90% CL

# Neutrino charge radius - results

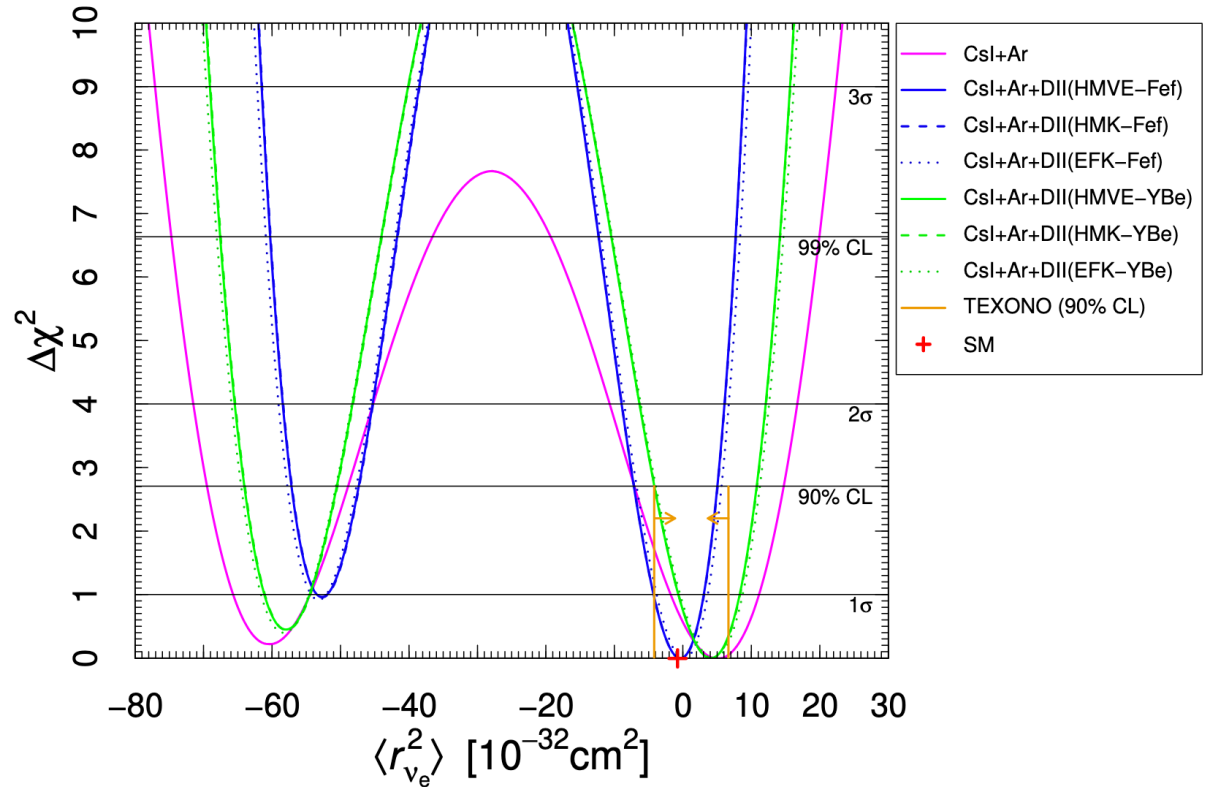
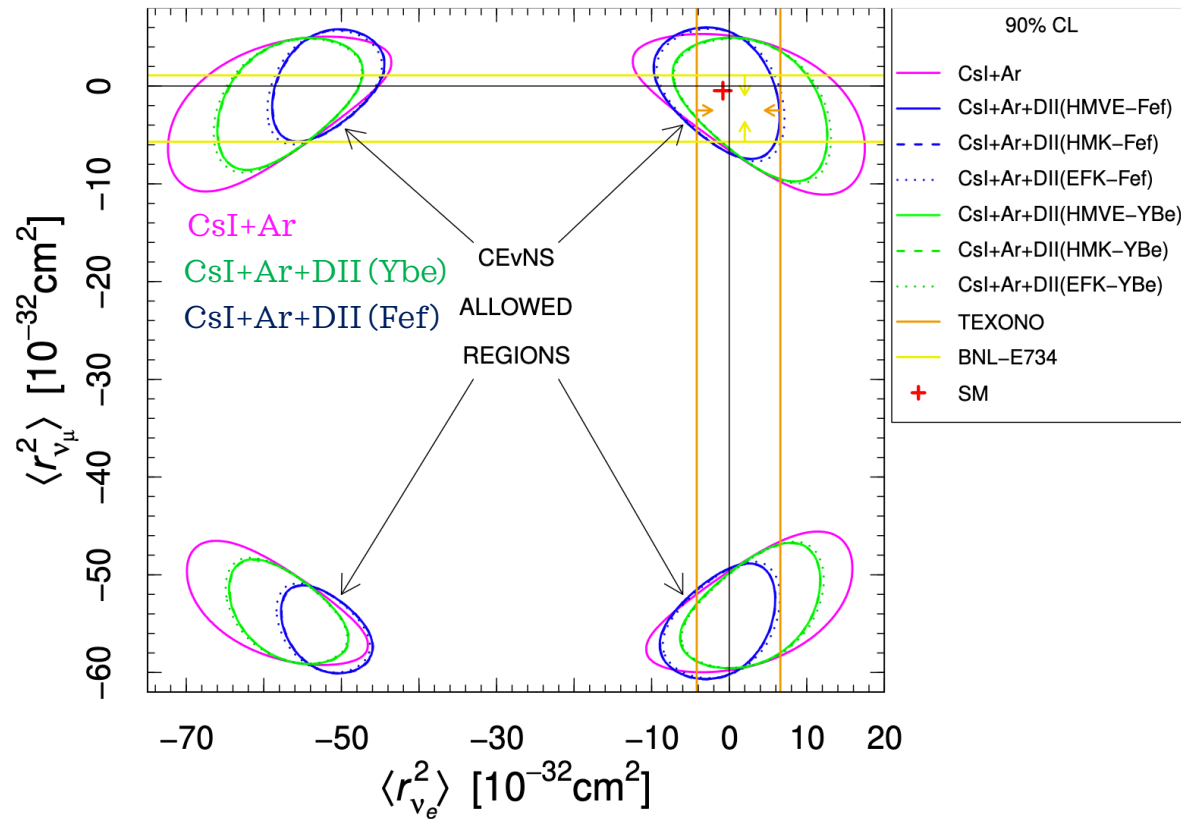
Assuming the **presence of transition CR**, **DRESDEN-II** can measure  $\langle r_{\nu_{ee}}^2 \rangle, |\langle r_{\nu_{e\mu}}^2 \rangle|, |\langle r_{\nu_{e\tau}}^2 \rangle|$  **COHERENT** also  $|\langle r_{\nu_{\mu\tau}}^2 \rangle|, \langle r_{\nu_{\mu\mu}}^2 \rangle$



- The CsI + Ar COHERENT combination is **vastly dominated by CsI**.
- **Dresden-II** and **CsI** datasets contribute with **roughly same precision**.
- **HMVE, HMK, EFK** different flux parametrization: practically independent, **highly sensitive to the QF used**.

# Neutrino charge radius - results

Assuming the **absence of transition CR**:  $\langle r_{\nu_e}^2 \rangle \equiv \langle r_{\nu_{ee}}^2 \rangle$  and  $\langle r_{\nu_\mu}^2 \rangle \equiv \langle r_{\nu_{\mu\mu}}^2 \rangle$



$-7.1 < \langle r_{\nu_e}^2 \rangle < 5$  [10<sup>-32</sup>cm<sup>2</sup>] **COHERENT + DRESDEN-II @ 90% CL**

- When using the Fef QF we **set a better upper bound with respect to that set by TEXONO** ( $6.6 \times 10^{-32} \text{cm}^2$ )
- No effect is found due to ES** on the neutrino CR, thus the results are independent of its inclusion

# NEUTRINO MAGNETIC MOMENT



# Neutrino magnetic moment- theory

- Predicted to be null for massless neutrinos.
- In minimal SM extensions in which neutrinos acquire Dirac masses through right-handed neutrinos the MM is given by

$$\mu_\nu = \frac{3 e G_F}{8\sqrt{2} \pi^2} m_\nu \simeq 3.2 \times 10^{-19} \left( \frac{m_\nu}{\text{eV}} \right) \mu_B \quad \boxed{=} \text{C. Giunti and A. Studenikin} \\ \text{Rev.Mod.Phys. 87 (2015) 531}$$

- Many BSM theories predict a MM larger than this. It adds incoherently to the cross-section:

**CEvNS:**  $\frac{d\sigma_{\nu\ell\mathcal{N}}^{\text{MM}}}{dT_{\text{nr}}}(E, T_{\text{nr}}) = \frac{\pi\alpha^2}{m_e^2} \left( \frac{1}{T_{\text{nr}}} - \frac{1}{E} \right) Z^2 F_Z^2(|\vec{q}|^2) \left( \frac{|\mu_{\nu\ell}|}{\mu_B} \right)^2$

**ES:**  $\frac{d\sigma_{\nu\ell\mathcal{A}}^{\text{ES, MM}}}{dT_e}(E, T_e) = Z_{\text{eff}}^{\mathcal{A}}(T_e) \frac{\pi\alpha^2}{m_e^2} \left( \frac{1}{T_e} - \frac{1}{E} \right) \left( \frac{|\mu_{\nu\ell}|}{\mu_B} \right)^2$

**Dependence on 1/T makes Dresden-II data really sensitive to it.**

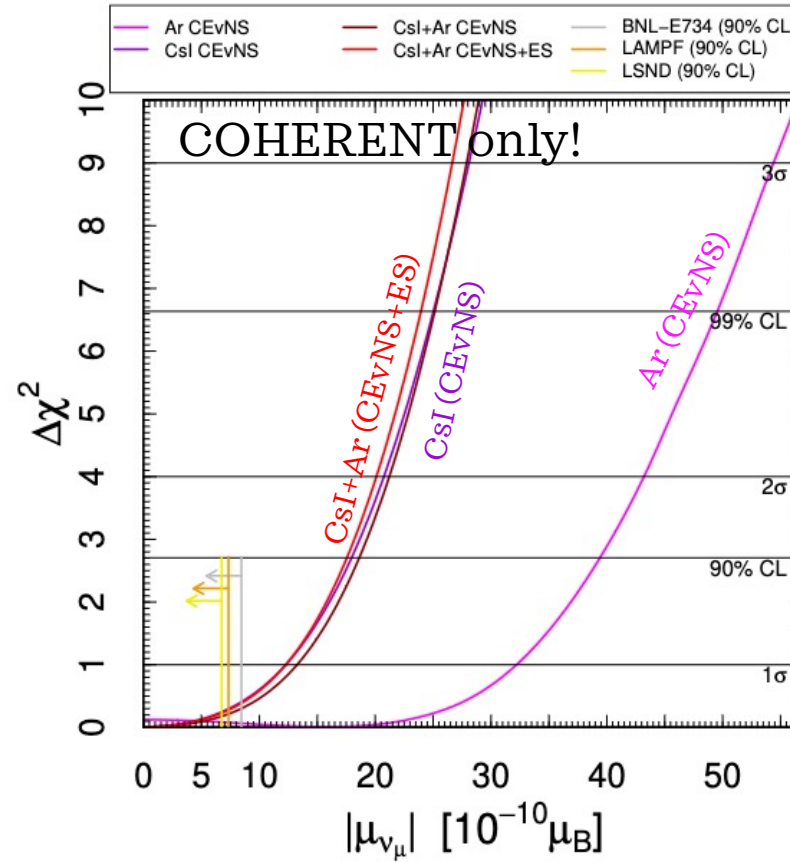
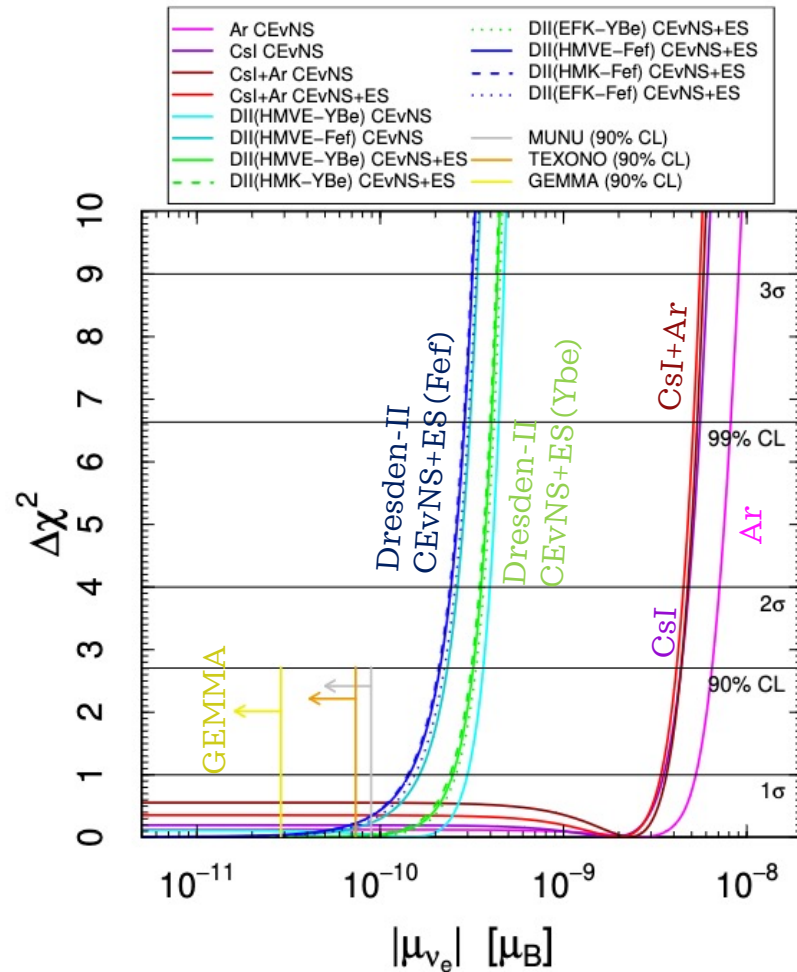
COHERENT allows to measure  $|\mu_{\nu_e}|$ , and  $|\mu_{\nu_\mu}|$ . Dresden-II allows to measure only  $|\mu_{\nu_e}|$ .

**Best limits @time of the paper:**  $|\mu_{\nu_e}| < 0.29 \times 10^{-10} \mu_B$  **GEMMA** @ 90% CL (reactor  $\bar{\nu}$ -e scattering) – also TEXONO and CONUS (CEvNS).  
 $|\mu_{\nu_\mu}| < 6.8 \times 10^{-10} \mu_B$  **LSND** @ 90% CL (accelerator  $\nu_e$ -e scattering).

➡ **End of 2022:** new best limits using solar  $\nu$ ES in **LZ** and **XENONnT**, see N. Cargioli talk on “*The role of the elastic neutrino-electron scattering in constraining the neutrino magnetic moment and millicharge using the LUX-ZEPLIN data*”.

$|\mu_\nu| < 6.4 \times 10^{-12} \mu_B$  [XENONnT]  $\boxed{=} \text{PRL 129, 161805 (2022)}$

# Neutrino magnetic moment results



$$|\mu_{\nu_e}| < 2.13 \times 10^{-10} \mu_B$$

Dresden-II (CevNS+ES)  
@90% CL

$$|\mu_{\nu_\mu}| < 18 \times 10^{-10} \mu_B$$

CsI (CevNS+ES)+Ar (CevNS+ES)  
@90% CL

- Not shown in the plot, LZ and XENONnT limits.
- Dresden-II data allow us to reduce the bound on  $|\mu_{\nu_e}|$  with respect to COHERENT by more than one order of magnitude.
- QF makes a factor of two difference, **Fef being more precise than YBe**
- The inclusion of **ES results in a marginal improvement** of the Dresden-II limits of about 10%.

# NEUTRINO ELECTRIC CHARGE



# Neutrino electric charge - theory

Even if neutrinos are considered as neutral particles, in some BSM theories they can acquire small electric charges (EC), sometimes called **millicharges**

**CE $\nu$ NS:** 
$$\frac{d\sigma_{\nu\ell-N}^{\text{CR}}}{dT_{\text{nr}}}(E, T_{\text{nr}}) = \frac{G_F^2 M}{\pi} \left(1 - \frac{MT_{\text{nr}}}{2E^2}\right) \left\{ \left[ (g_V^p - \tilde{Q}_{\ell\ell}) Z F_Z(|\vec{q}|^2) + g_V^n N F_N(|\vec{q}|^2) \right]^2 + Z^2 F_Z^2(|\vec{q}|^2) \sum_{\ell' \neq \ell} |\tilde{Q}_{\ell\ell'}|^2 \right\}$$

with  $Q_{\ell\ell'} = \frac{2\sqrt{2}\pi\alpha}{G_F q^2} q_{\nu\ell\ell'}$

$q^2 = -2MT_{\text{nr}}$

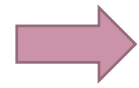
Helps to set more stringent limits with reactor experiments (low  $q^2$  and low en. threshold) and with Ar vs CsI (smaller Ar mass).

**ES:** 
$$\left( \frac{d\sigma_{\nu\ell-A}^{\text{ES,EC}}}{dT_e} \right)_{\text{SM}+Q} = \left( \frac{d\sigma_{\nu\ell-A}^{\text{ES,EC}}}{dT_e} \right)_{\text{SM}} + \sum_{\ell' \neq \ell} Z_{\text{eff}}^A(T_e) \frac{\pi\alpha^2}{m_e T_e^2} \left[ 1 + \left(1 - \frac{T_e}{E}\right)^2 - \frac{m_e T_e}{E^2} \right] |q_{\nu\ell\ell'}|^2$$

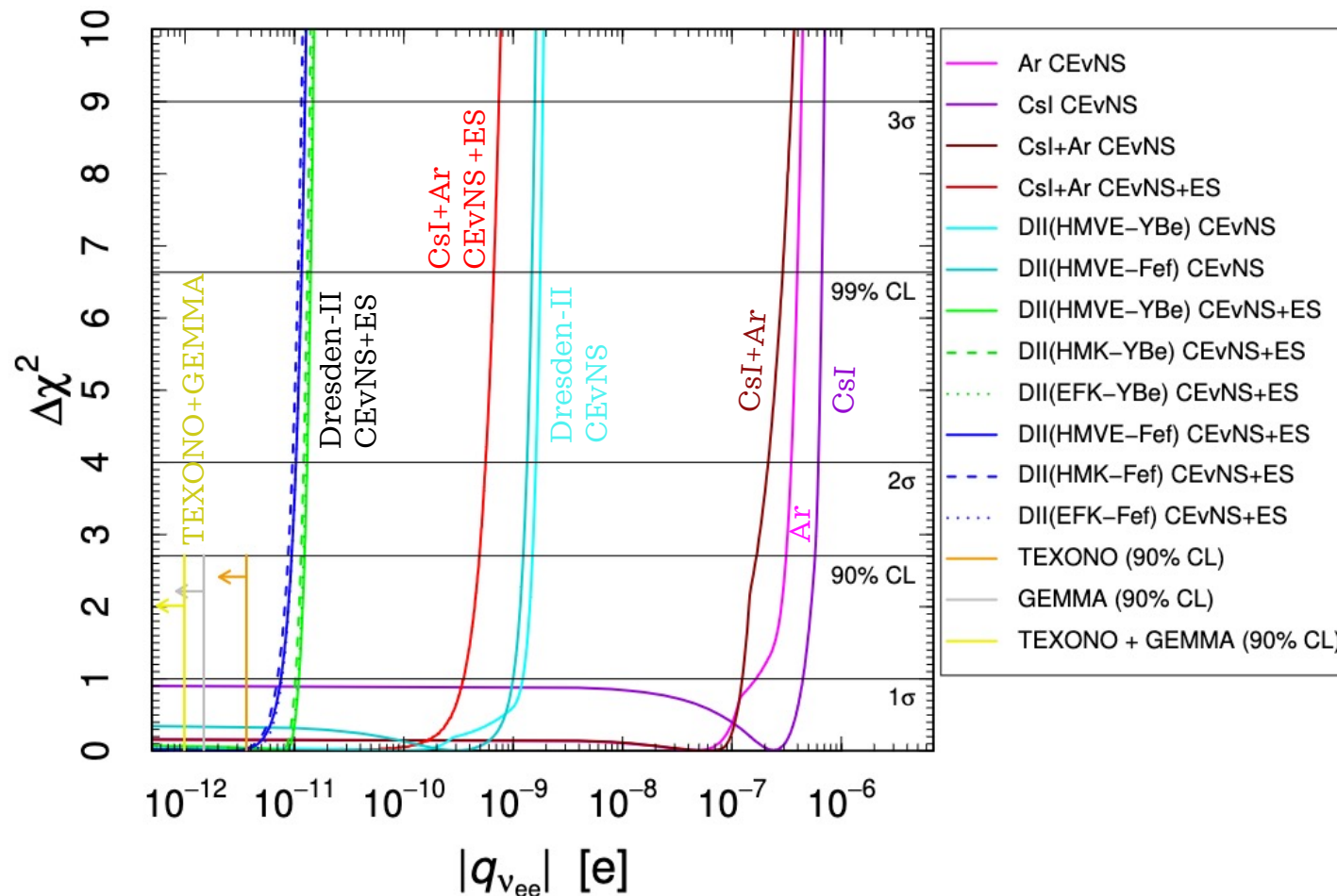
Dependence on  $1/T_e^2$  makes ES data really sensitive to it.

COHERENT allows to measure  $q_{\nu\mu\mu}, |q_{\nu\mu\tau}|, q_{\nu ee}, |q_{\nu e\mu}|, |q_{\nu e\tau}|$ . Dresden-II allows to measure the last 3.

**Best limits @time of the paper:**  $q_{\nu ee}$  by GEMMA (reactor  $\bar{\nu}$ -e scattering) and TEXONO (accelerator  $\nu_e$ -e scattering)+CONUS.  
 $q_{\nu\mu\mu}$  by XMASS-I (solar  $\nu$ -e scattering) and LSND (accelerator  $\nu_e$ -e scattering).

 **End of 2022:** new best limits using solar  $\nu$ ES in LZ, see N. Cargioli talk on “*The role of the elastic neutrino-electron scattering in constraining the neutrino magnetic moment and millicharge using the LUX-ZEPLIN data*”

 PRD 107, 053001 (2023)



**CEvNS + ES:**  $-9.3 < q_{v_{ee}} < 9.5 [10^{-12} e]$

- Not shown in the plot:  $|q_{v_{ee}}| < 1.5 \times 10^{-13} e$  [**LZ**];  $\boxed{=}$  PRD 107, 053001 (2023)
- The latter has been obtained using Equivalent Photon Approximation (EPA) approach (similar to RRPA for EC) that provides a larger cross-section especially at sub-keV energies wrt FEA;
- Our result can be considered as conservative.

# NEUTRINO ELECTRIC CHARGE - RESULTS

- Despite having more CsI statistics, the **low Ar mass permits to achieve stronger constraints** with Ar

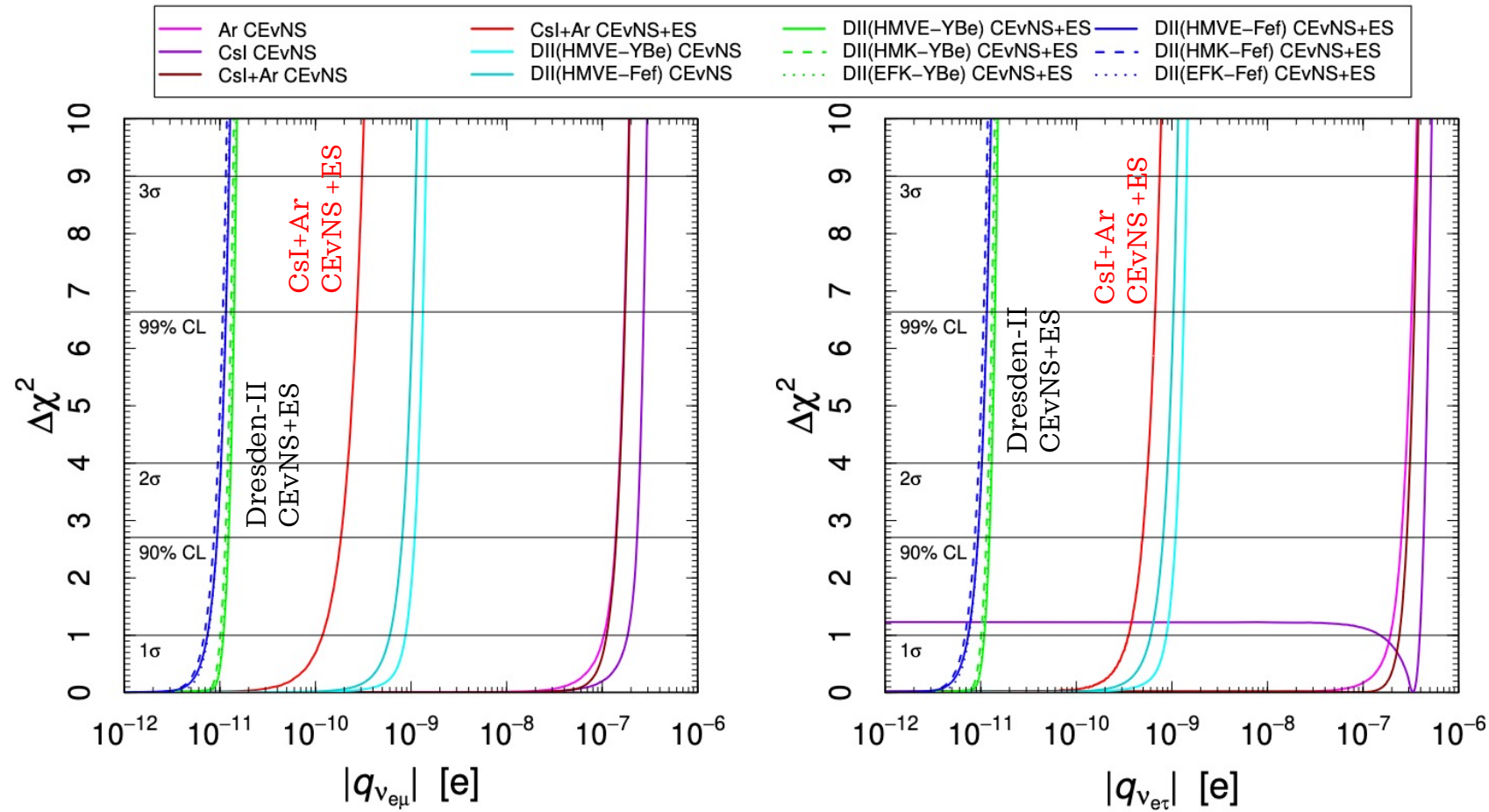
- Due to the low  $q^2$ , **DRESDEN-II data improves COHERENT limits** by more than 2 orders of magnitude.



Combination completely dominated by DRESDEN-II

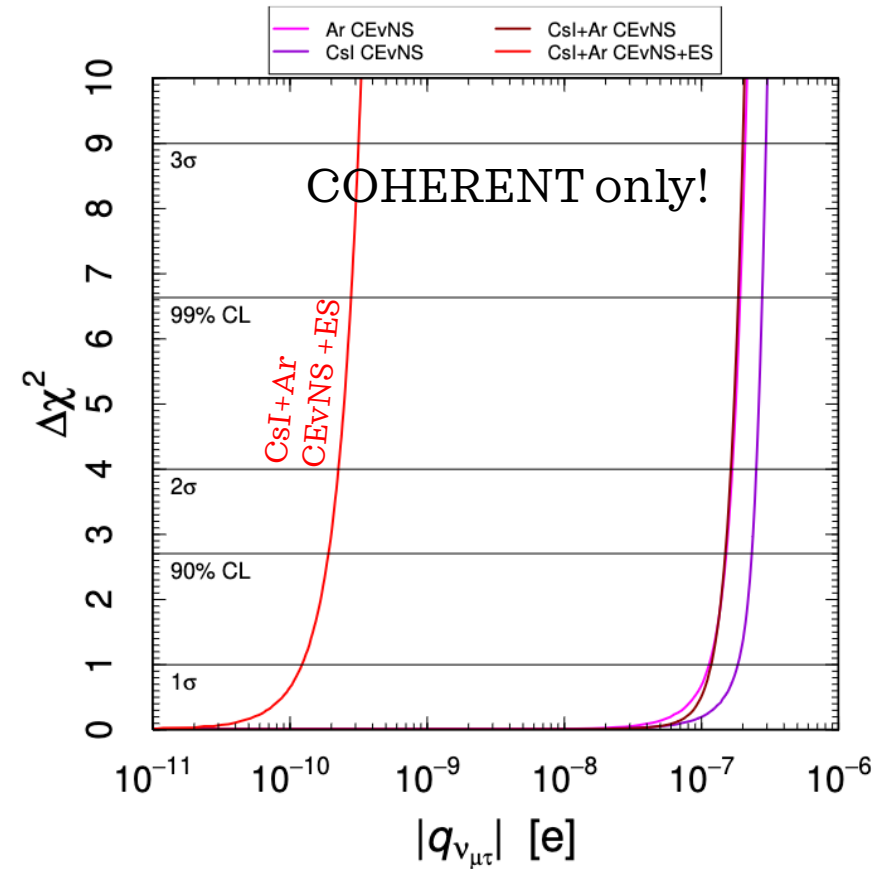
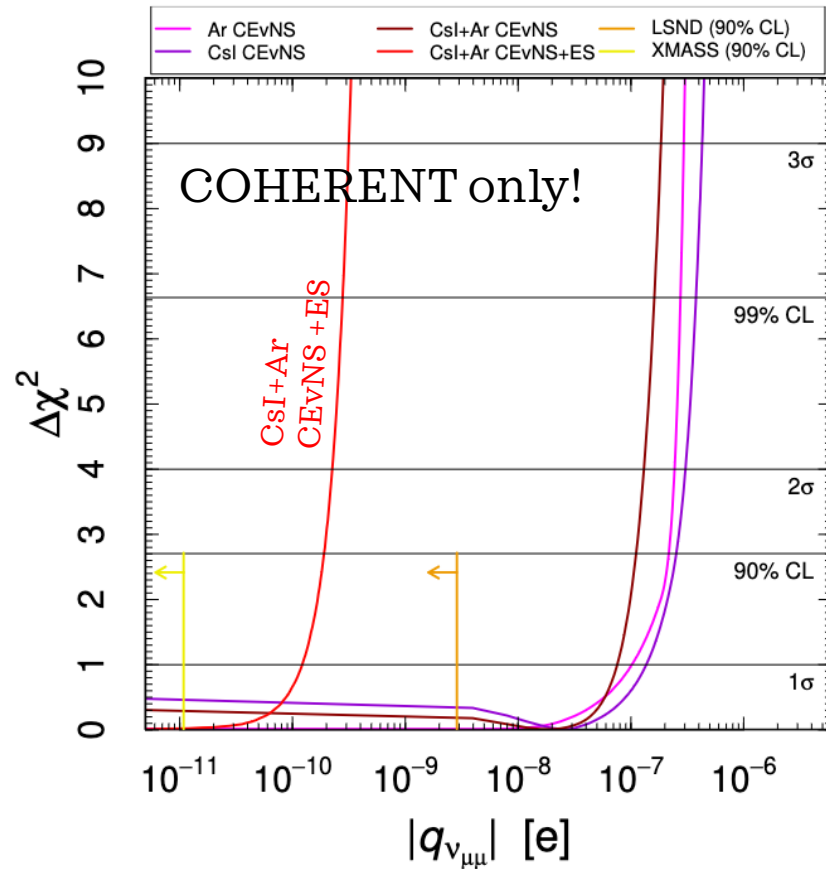
- The contribution of the **Electron Scattering** (ES) improves COHERENT and DRESDEN-II limits by more than 2 orders of magnitude

# Neutrino electric charge - results



Also in this case the contribution of Dresden-II + ES dominates.

# Neutrino electric charge - results



- Competitive results on  $|q_{\nu\mu\mu}|$  wrt XMASS and better than LSND  
 [PLB 809 (2020) 135741] [PRD 63 (2001) 112001]
- Not shown in the plot:  $|q_{\nu\mu\mu}| < 3.1 \times 10^{-13} e$  [LZ]; [PRD 107, 053001 (2023)]

- Only existing laboratory bound.**



# Conclusions

- COHERENT and Dresden-II (reactor) data shows **good complementarity** in constraining neutrino properties
- Concerning Dresden-II the impact of the various  $\nu$  fluxes is negligible, while the QF results in large differences (not even considering the Lindhard model): **necessity to further discuss the QF at low energy for germanium.**
- **Impact of elastic neutrino-electron scattering** allows us to tighten significantly the bounds on  $\nu$  magnetic moment and millicharge.
- **Competitive limits on the  $\nu$  millicharge and charge radii.**
- CEvNS process prove to be once again a **spectacular window** to test many and diverse sector with very competitive precision.

# BACKUP

# WHAT CAN WE LEARN FROM CE $\nu$ NS?

$$\begin{array}{c}
 \text{Neutrino energy} \quad \text{Mass of the nucleus} \quad \text{SM vector proton coupling} \quad \boxed{\begin{array}{l} g_V^p(\nu_e) = 0.0382 \\ g_V^p(\nu_\mu) = 0.0300 \\ g_V^n = -0.5117^* \end{array}} \quad \text{SM vector neutron coupling} \\
 \downarrow \quad \downarrow \quad \downarrow \quad \downarrow \quad \downarrow \\
 \frac{d\sigma^{CE\nu NS}(E_\nu, T_{nr})}{dT_{nr}} \cong \frac{G_F^2 m_N}{\pi} \left(1 - \frac{m_N T_{nr}}{2E_\nu^2}\right) \left[ g_V^p \left( \sin^2(\vartheta_W) \right) Z F_Z(|\vec{q}|^2) + g_V^n N F_N(|\vec{q}|^2) \right]^2 \\
 \uparrow \quad \uparrow \quad \uparrow \quad \uparrow \quad \uparrow \\
 \text{Nuclear recoil energy} \quad \text{Weinberg angle} \quad \text{Proton Form Factor} \quad \text{Neutron Form Factor}
 \end{array}$$

\* when taking into account radiative corrections, see JHEP09(2022)164

# WHAT CAN WE LEARN FROM CE $\nu$ NS?

See M. Atzori-Corona, V. De Romeri and A. Majumdar talks

Neutrino energy  
Mass of the nucleus

SM vector proton coupling

**New  $\nu$  interaction**

SM vector neutron coupling

**In this talk!**  
 **$\nu$  EM properties**

See also N. Cargioli and D. Papoulias' talks

$$\frac{d\sigma^{CE\nu NS}(E_\nu, T_{nr})}{dT_{nr}} \cong \frac{G_F^2 m_N}{\pi} \left(1 - \frac{m_N T_{nr}}{2E_\nu^2}\right) \left[ g_V^p \left( \sin^2(\vartheta_W) \right) Z F_Z(|\vec{q}|^2) + g_V^n N F_N(|\vec{q}|^2) \right]^2 + \dots$$

Nuclear recoil energy

Weinberg angle

Proton Form Factor

Neutron Form Factor

**EW precision**

**Nuclear physics**

See M. Cadeddu and D. Papoulias' talks

# The $Z_{\text{eff}}$ term

$Z_{\text{eff}}^{\text{Cs}} =$	55,	$T_e > 35.99 \text{ keV}$	$Z_{\text{eff}}^{\text{I}} =$	53,	$T_e > 33.17 \text{ keV}$
	53,	$35.99 \text{ keV} \geq T_e > 5.71 \text{ keV}$		51,	$33.17 \text{ keV} \geq T_e > 5.19 \text{ keV}$
	51,	$5.71 \text{ keV} \geq T_e > 5.36 \text{ keV}$		49,	$5.19 \text{ keV} \geq T_e > 4.86 \text{ keV}$
	49,	$5.36 \text{ keV} \geq T_e > 5.01 \text{ keV}$		47,	$4.86 \text{ keV} \geq T_e > 4.56 \text{ keV}$
	45,	$5.01 \text{ keV} \geq T_e > 1.21 \text{ keV}$		43,	$4.56 \text{ keV} \geq T_e > 1.07 \text{ keV}$
	43,	$1.21 \text{ keV} \geq T_e > 1.07 \text{ keV}$		41,	$1.07 \text{ keV} \geq T_e > 0.93 \text{ keV}$
	41,	$1.07 \text{ keV} \geq T_e > 1 \text{ keV}$		39,	$0.93 \text{ keV} \geq T_e > 0.88 \text{ keV}$
	37,	$1 \text{ keV} \geq T_e > 0.74 \text{ keV}$		35,	$0.88 \text{ keV} \geq T_e > 0.63 \text{ keV}$
	33,	$0.74 \text{ keV} \geq T_e > 0.73 \text{ keV}$		31,	$0.63 \text{ keV} \geq T_e > 0.62 \text{ keV}$
	27,	$0.73 \text{ keV} \geq T_e > 0.23 \text{ keV}$		25,	$0.62 \text{ keV} \geq T_e > 0.19 \text{ keV}$
	25,	$0.23 \text{ keV} \geq T_e > 0.17 \text{ keV}$		23,	$0.19 \text{ keV} \geq T_e > 0.124 \text{ keV}$
	23,	$0.17 \text{ keV} \geq T_e > 0.16 \text{ keV}$		21,	$0.124 \text{ keV} \geq T_e > 0.123 \text{ keV}$
	19,	$T_e < 0.16 \text{ keV}$		17,	$T_e < 0.123 \text{ keV}$

**Table 1.** The effective electron charge of the target atom,  $Z_{\text{eff}}^{\text{A}}(T_e)$ , for Cs and I.

$Z_{\text{eff}}^{\text{Ge}} =$	32,	$T_e > 11.103 \text{ keV}$
	30,	$11.103 \text{ keV} \geq T_e > 1.4146 \text{ keV}$
	28,	$1.4146 \text{ keV} \geq T_e > 1.2481 \text{ keV}$
	26,	$1.2481 \text{ keV} \geq T_e > 1.217 \text{ keV}$
	22,	$1.217 \text{ keV} \geq T_e > 0.1801 \text{ keV}$
	20,	$0.1801 \text{ keV} \geq T_e > 0.1249 \text{ keV}$
	18,	$0.1249 \text{ keV} \geq T_e > 0.1208 \text{ keV}$
	14,	$0.1208 \text{ keV} \geq T_e > 0.0298 \text{ keV}$
	10,	$0.0298 \text{ keV} \geq T_e > 0.0292 \text{ keV}$
	4,	$T_e \leq 0.0292 \text{ keV}$

**Table 2.** The effective electron charge of the target atom,  $Z_{\text{eff}}^{\text{A}}(T_e)$ , for Ge.

Specific for each atom, obtained using edge energies from photo-absorption data.

 A. Thompson et al., X-ray data booklet, <https://xdb.lbl.gov/>, Lawrence Berkeley National Laboratory, U.S.A. (2009)

# The antineutrino flux

In order to derive the antineutrino spectra  $dN_{\bar{\nu}}/dE$  from the Dresden-II reactor we have considered three different parametrizations, obtained by combining four different predictions for specific energy ranges. In particular, the neutrino spectra are built by combining the expected spectra for antineutrino energies above 2 MeV from either ref. [72] or ref. [73], that we indicate as HM and EF, respectively, with the low energy part determined by ref. [74] and refs. [75, 76], that we indicate as VE and K, respectively. In this way, three different combinations are obtained, to which we will refer to as HMVE, EFK, and HMK. These spectra are obtained from the weighted average of the antineutrino fluxes from four main fission isotopes, namely  $^{235}\text{U}$ ,  $^{239}\text{Pu}$ ,  $^{238}\text{U}$  and  $^{241}\text{Pu}$ . In the K prediction [75, 76], the contribution at low energies from radiative neutron capture on  $^{238}\text{U}$  is also taken into account. The latter has the effect to enhance the spectrum for neutrino energies below  $\sim 1$  MeV. In all cases, we set the spectra to zero above 10 MeV. The neutrino spectra for reactor antineutrinos have been normalized to the antineutrino flux estimate reported in ref. [36] and corresponding to  $\Phi_{\text{est}} = 4.8 \times 10^{13} \text{ cm}^{-2}\text{s}^{-1}$ , that has been determined considering a reactor power  $P = 2.96 \text{ GW}_{\text{th}}$  and a reactor-detector distance of  $L = 10.39 \text{ m}$  [36].

# The charge radii summary

Process	Collaboration	Limit [ $10^{-32} \text{ cm}^2$ ]	C.L.	Ref.
Reactor $\bar{\nu}_e$ -e	Krasnoyarsk	$ \langle r_{\nu_e}^2 \rangle  < 7.3$	90%	[94]
	TEXONO	$-4.2 < \langle r_{\nu_e}^2 \rangle < 6.6$	90%	[91] <sup>a</sup>
Accelerator $\nu_e$ -e	LAMPF	$-7.12 < \langle r_{\nu_e}^2 \rangle < 10.88$	90%	[95] <sup>a</sup>
	LSND	$-5.94 < \langle r_{\nu_e}^2 \rangle < 8.28$	90%	[96] <sup>a</sup>
Accelerator $\nu_\mu$ -e and $\bar{\nu}_\mu$ -e	BNL-E734	$-5.7 < \langle r_{\nu_\mu}^2 \rangle < 1.1$	90%	[92] <sup>a, b</sup>
	CHARM-II	$ \langle r_{\nu_\mu}^2 \rangle  < 1.2$	90%	[97] <sup>a</sup>
COHERENT + Dresden-II	w/o transition CR	$-7.1 < \langle r_{\nu_e}^2 \rangle < 5$	90%	This work <sup>c</sup>
	w transition CR	$-56 < \langle r_{\nu_e}^2 \rangle < 5$	90%	This work <sup>c</sup>
COHERENT + Dresden-II	w/o transition CR	$-5.9 < \langle r_{\nu_\mu}^2 \rangle < 4.3$	90%	This work <sup>c</sup>
	w transition CR	$-58.2 < \langle r_{\nu_\mu}^2 \rangle < 4.0$	90%	This work <sup>c</sup>

<sup>a</sup>Corrected by a factor of two due to a different convention, see ref. [21].

<sup>b</sup>Corrected in ref. [93].

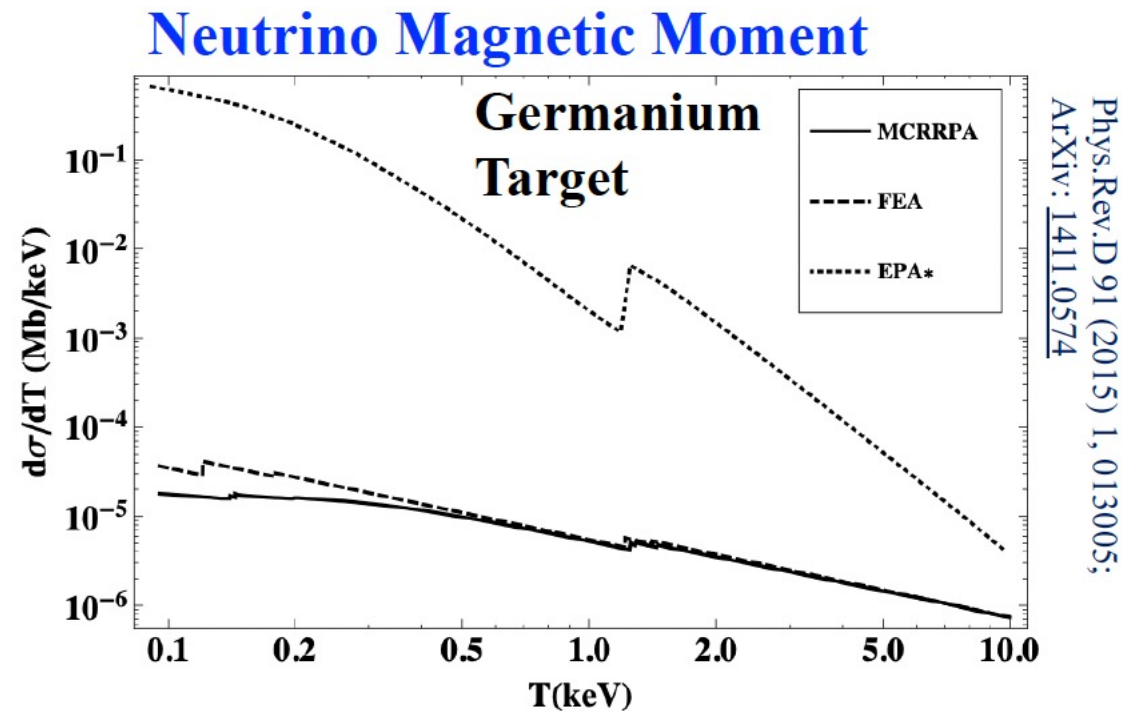
<sup>c</sup>Using the Fef quenching factor.

**Table 7.** Experimental limits for the neutrino charge radii.

# EPA, FEA, and RPPA comparison for MM

**RRPA**: Relativistic Random-Phase Approximation, ab-initio approach able to improve the description of the atomic many-body effects

**EPA**: Equivalent Photon Approximation, relates the ionization cross section to the photo-absorption one



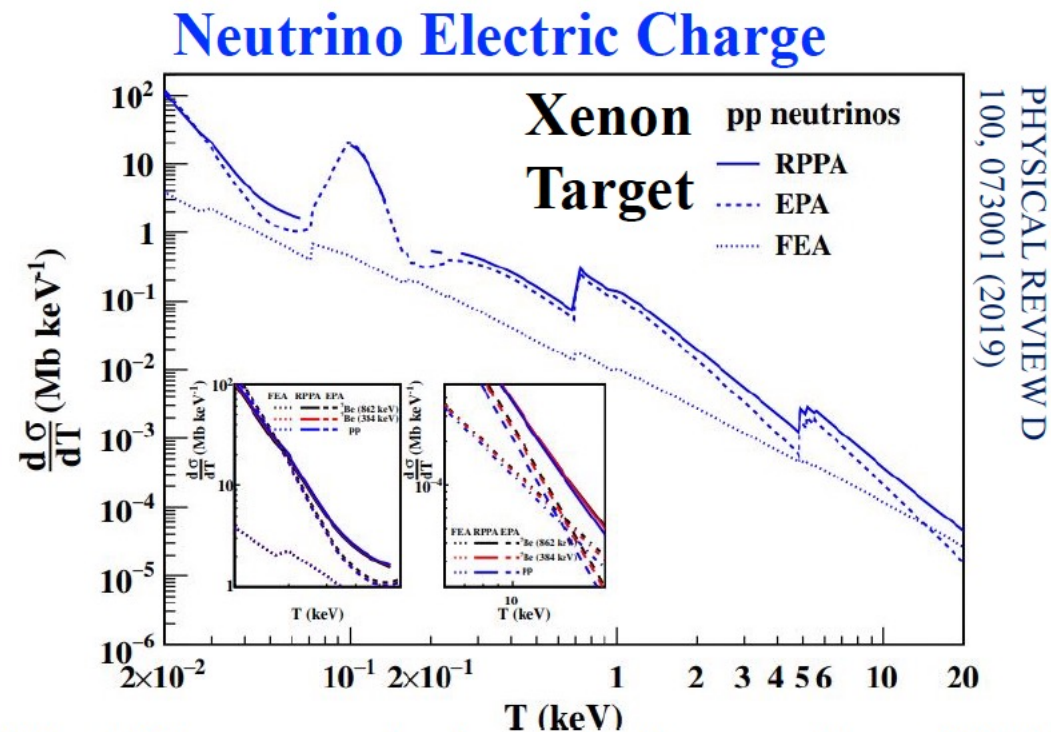
The FEA approach gives similar results to RRPA for the MM, while **EPA doesn't work well**

Taken from N. Cargioli

# EPA, FEA, and RPPA comparison for EC

**RRPA**: Relativistic Random-Phase Approximation, ab-initio approach able to improve the description of the atomic many-body effects

**EPA**: Equivalent Photon Approximation, relates the ionization cross section to the photo-absorption one



The EPA approach gives similar results to RRPA for the EC, while **FEA doesn't work well**

Taken from N. Cargioli

# Germanium quenching factor

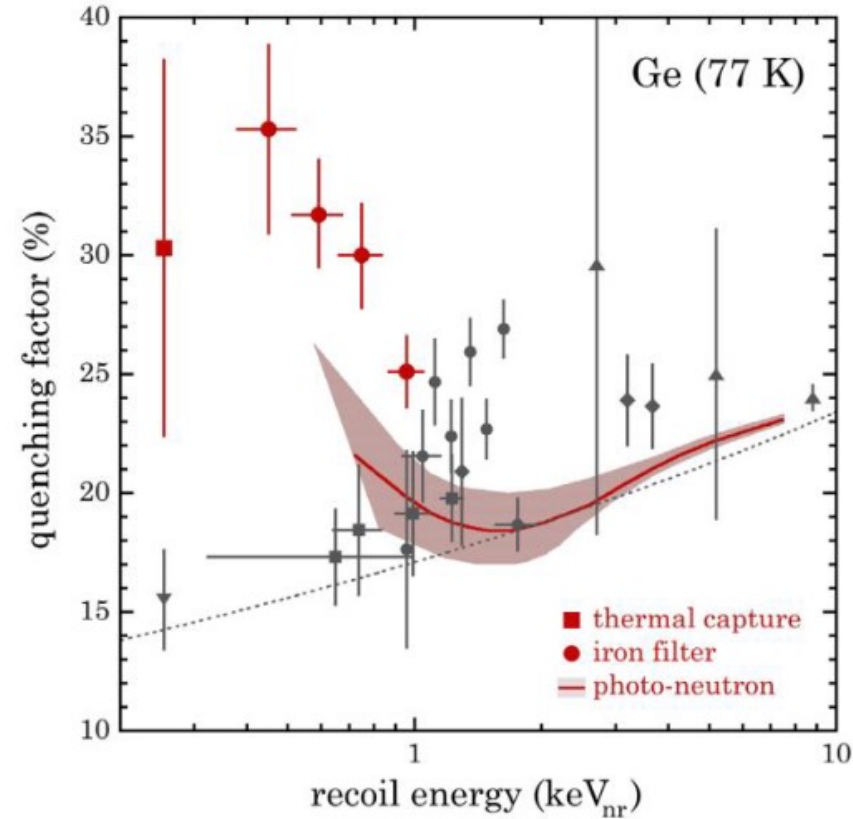


FIG. 9. Present QF results, labeled by calibration technique. A red band shows the 95% C.L. region for the model-independent fit of Fig. 2. A dotted line is the Lindhard model with a default germanium value of  $k = 0.157$  [22]. Previous measurements are shown in gray: circles [57], squares [9,25], diamonds [65], triangles [66], and inverted triangle [51].